

**DEVELOPMENT AND STUDY OF MOLTEN
SALT ELECTRODEPOSITION SYSTEM USING
DIFFERENT VOLTAGE FEEDING**

MIRON GAKIM



UMS
UNIVERSITI MALAYSIA SABAH

**THESIS SUBMITTED IN FULFILLMENT FOR
THE DEGREE OF
DOCTOR OF PHILOSOPHY**

UNIVERSITI MALAYSIA SABAH

**FACULTY OF ENGINEERING
UNIVERSITI MALAYSIA SABAH
2018**

UNIVERSITI MALAYSIA SABAH

BORANG PENGESAHAN STATUS TESIS

JUDUL : **DEVELOPMENT AND STUDY OF MOLTEN SALT ELECTRODEPOSITION SYSTEM USING DIFFERENT VOLTAGE FEEDING**

IJAZAH: **DOKTOR FALSAFAH (KEJURUTERAAN MEKANIKAL)**

Saya **MIRON GAKIM**, Sesi **2012-2018**, mengaku membenarkan tesis Doktor ini disimpan di Perpustakaan Universiti Malaysia Sabah dengan syarat-syarat kegunaan seperti berikut:

1. Tesis ini adalah hak milik Universiti Malaysia Sabah.
2. Perpustakaan Universiti Malaysia Sabah dibenarkan membuat salinan untuk tujuan pengajian sahaja.
3. Perpustakaan dibenarkan membuat salinan tesis ini sebagai bahan pertukaran antara institusi pengajian tinggi.
4. Sila tandakan (/):

SULIT


(Mengandungi maklumat yang berdarjah keselamatan atau kepentingan Malaysia seperti yang termaktub di dalam AKTA RAHSIA 1972)

TERHAD

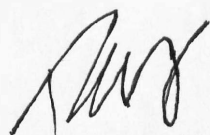
(Mengandungi maklumat TERHAD yang telah ditentukan oleh organisasi/badan di mana penyelidikan dijalankan)

TIDAK TERHAD


MIRON GAKIM
PK1211013T

Disahkan Oleh,

NURULAIN BINTI ISMAIL
PUSTAKAWAN KANAN
UNIVERSITI MALAYSIA SABAH
(Tandatangan Pustakawan)

Tarikh : 28th SEPTEMBER 2018


(Dr. Nancy Julius Siambun)
Penyelia

CERTIFICATION

NAME : MIRON GAKIM
MATRIC NO : PK1211013T
**TITLE : DEVELOPMENT AND STUDY OF MOLTEN SALT
ELECTRODEPOSITION SYSTEM USING DIFFERENT
VOLTAGE FEEDING**
**DEGREE : DOCTOR OF PHILOSOPHY
(MECHANICAL ENGINEERING)**
VIVA DATE : 10TH JULY 2018

CERTIFIED BY

Signature

- 1. SUPERVISOR**
DR. NANCY JULIUS SIAMBUN



UMS
UNIVERSITI MALAYSIA SABAH

A handwritten signature in black ink, appearing to read "Nancy Julius Siambun", is written over a horizontal line.

ACKNOWLEDGEMENT

I wish to express my deepest gratitude to God who gave me the grace, health and the means of sustenance with which I was able to undertake doctorate studies. He has intervened in my life in positive ways in years past and He has shown Himself as a reliable and present help in time of need.

I would like to express my sincere gratitude to my supervisor, Dr. Nancy Julius Siambun for the continuous support of my PhD study and research, for her patience, guidance and motivation. Without her sharing and guidance of knowledge, this thesis would not have been possible.

I am indebted to Biotechnology Research Institute of Universiti Malaysia Sabah (UMS), Fakulti Pembuatan Universiti Teknikal Malaysia Melaka (UTeM) and Universiti Technology Malaysia (UTM) providing me to use their instruments for the analysis. I also wish to thank Ministry of Higher Education (MOHE) for providing a financial support through the programme MyBrain15.

I would also like to thank the fellow staffs and lab mates in Fakulti Kejuruteraan (FKJ) for their idea and encouragement. They are Mr. Jester Ling Lih Jie, Miss Karen Wong Min Jin, Mr. Valerian Victor Kong, Dayang Nurhazwani Kasim, Maisarah Binti Nasharudin and Mr. Afenley Inggui. I also like to express my appreciation to Mdm. Nurul Fatehah bt Ansari for thesis proofreading.

Also, big thanks to all examiners Prof. Madya Dr. Coswald Stephen @ Mohd. Nasri, Prof. Dr. Seock-Sam Kim, and Prof. Madya Ir. Dr. Mohd Asyadi `Azam bin Mohd Abid for very constructive comments toward this thesis work.

I would finally like to thank my parent for their love, pray and encouragement has strengthened me with full of hope and confidence to finish this project.

MIRON GAKIM
28th SEPTEMBER 2018

ABSTRACT

Electrochemical conversion of CO_2 into solid carbon is one of the conversion techniques that had been developed which contributes in the carbon capture and utilisation (CCU). The electro reduction process in molten alkali/earth alkali carbonate salt reduces carbonate ion to form solid carbon and alkali/earth alkali metal oxide. Then, the metal oxide reacts with CO_2 to reform carbonate ion. This cycle is called the fixation process. However, at a low operating temperature, the charge transfer of the electrolysis process was low and experience current drop after the operation period was prolonged. These leads to the low production rate of solid carbon. The factor that caused the low charge transfer has been described in this thesis. The motivation of study is to improve the charge transfer at operating temperature range 550 - 570 °C and driven at constant voltage 4V which was previously claimed could promotes high current efficiency at this temperature. Therefore, the main objective was to instigate an experimental understanding of electrolysis process on carbon electrodeposition under different voltage feeding. The voltage feeder was invented as to provide electrochemical agitation in the electrolysis system. The electrolysis system with Double Pole Double (DPDT) switch was developed in the electrolysis system as the voltage feeder. The agitation was done by changing the DC current flow manually to drive the electrolysis process. The gated pulse and alternate voltage feeding operation was described in this thesis. The effect of the voltage feeding on electrolysis in molten $\text{Li}_2\text{CO}_3 - \text{Na}_2\text{CO}_3 - \text{K}_2\text{CO}_3$ with mole ratio (0.44:0.30:0.26) and salt mixture $\text{CaCO}_3 - \text{Li}_2\text{CO}_3 - \text{LiCl}$ with mole ratio (0.09:0.28:0.63) was studied. The effect of voltage feeding on total charge transfer and carbon yield was studied. The succeeded electrodeposited products were characterised through EA, SEM-EDX, TEM, XRD and ATR-FTIR. The results showed the total charge transfer under alternate voltage feeding was extremely high compared to gated pulse and continuous voltage feeding which leads to high carbon deposition rate. Through EA characterisation, it was found that the produced sample under different voltage feeding exhibit higher than 60% of carbon content, therefore the deposited samples were carbon dominant. However, approximately 12% of carbon content was observed for samples produced in $\text{Li}_2\text{CO}_3 - \text{Na}_2\text{CO}_3 - \text{K}_2\text{CO}_3$ under alternate voltage feeding. Under the SEM-EDX analysis, the observed essential carbon structure was found differed based on the types of the salt bath and also effected with voltage feeder. Carbon nanotubes structure was seen in the samples prepared under alternate voltage feeding for both salt mixtures. TEM analysis confirmed the existence of carbon nanotubes. Through XRD analysis, the obtained dominant carbon deposition was amorphous type. Due to the corrosion of the electrode, crystallite of metallic compound was significantly observed for sample prepared using alternate voltage feeding in molten mixture $\text{Li}_2\text{CO}_3 - \text{Na}_2\text{CO}_3 - \text{K}_2\text{CO}_3$. The functional group on the surface of the sample was hard to determined due to the noise from the strong IR spectra of intrinsic diamond peak from the FTIR probe at region 1700 – 2700 cm^{-1} . In alternate voltage feeding, the charge transfer in the process was high, however the carbon yield was relatively low. Henceforth, it leads to low current efficiency, and therefore high energy density was necessary to produce carbon. It was found that with the increased of carbon loses during the process, it reduced the current efficiency and thus increased the energy consumption.

ABSTRAK

PEMBANGUNAN DAN KAJIAN SISTEM ELEKTROENAPAN LEBURAN GARAM MENGGUNAKAN PEMBEZA PACUAN VOLTAN

Penukaran CO₂ kepada karbon melalui kaedah elektrokimia adalah salah satu teknik yang telah dimajukan dan mampu menyumbangkan kepada penangkapan dan penggunaan karbon (CCU). Proses elektro penurunan dalam leburan garam karbonat alkali/bumi alkali akan melibatkan penurunan ion karbonat untuk membentuk pepejal karbon dan oksida logam alkali/alkali bumi. Kemudian, oksida logam ini bertindak balas terhadap CO₂ untuk membentuk semula ion karbonat. Kitaran ini disebut sebagai proses penetapan. Walau bagaimanapun, pada operasi elektrolisis suhu yang rendah, pemindahan cas elektrolisis adalah lemah dan mengakibatkan kadar penghasilan pepejal karbon yang perlahan. Motivasi kajian adalah untuk meningkatkan jumlah perpindahan cas pada julat suhu 550 - 570 °C dan dipacu pada voltan tetap 4 DCV, dimana voltan ini telah dilaporkan mampu memberi kecekapan arus yang tinggi pada julat suhu tersebut. Oleh itu, objektif utama kajian ini adalah untuk meneliti proses elektrolisis menerusi pembeza pacuan masukan voltan. Pacuan masukan voltan telah direka untuk memberikan kesan agitasi elektrokimia dalam sistem elektrolisis. Sistem DPDT (suis dua kutub dua arah) diperkenalkan dalam sistem elektrolisis sebagai pemacu masukan voltan. Pengagitasian telah dibuat dengan mengubah aliran arus DC secara manual yang memacu proses elektrolisis menerusi DPDT. Operasi pacuan voltan nadi berpagar dan pola berganti telah dijelaskan dalam tesis ini. Kesan pacuan voltan pada elektrolisis dalam campuran leburan garam Li₂CO₃ – Na₂CO₃ – K₂CO₃ (nisbah mol 0.44:0.30:0.26) dan campuran leburan garam CaCO₃ – Li₂CO₃ – LiCl (nisbah mol 0.09:0.28:0.63) telah dipelajari. Pencirian sifat produk enapan bagi setiap pacuan voltan telah diuji melalui EA, SEM-EDX, TEM, XRD, dan ATR-FTIR. Hasil ujikaji menunjukkan jumlah pemindahan cas yang tinggi berlaku menerusi pacuan voltan pola berganti berbanding pacuan voltan nadi berpagar dan pacuan voltan berterusan. Menerusi pencirian EA, sampel enapan bagi setiap pacuan voltan mengandungi 60 % kandungan karbon kecuali sampel yang dijana dalam leburan garam Li₂CO₃ – Na₂CO₃ – K₂CO₃ menerusi pacuan polar berganti iaitu kandungan karbon hanya sekitar 12 %. Analisis SEM-EDX mendapati struktur-struktur karbon yang terhasil adalah bergantung pada jenis leburan garam dan turut dipengaruhi dengan voltan yang dipacu. Pacuan voltan pola berganti mampu menghasilkan struktur tiub nano karbon dalam sampel enapan bagi kedua-dua jenis garam yang digunakan. Analisis TEM telah memastikan kehadiran tiub nano karbon. Menerusi analisis XRD, sampel karbon adalah jenis armofofos. Kesan daripada kakisan pada electrode, kehadiran struktur komposisi logam telah dikesan dalam sampel enapan voltan pola berganti dalam Li₂CO₃ – Na₂CO₃ – K₂CO₃. Kumpulan berfungsi dalam sampel karbon tidak kelihatan selain spektra yang menunjuk sisa penyerapan struktur berlian daripada prob FTIR sekitar 1700 – 2700 cm⁻¹. Perpindahan cas menerusi pacuan pola berganti adalah tinggi namun relatifnya terhadap penghasilan karbon adalah rendah. Ini mengakibatkan kecekapan arus rendah dan seterusnya mengakibatkan penggunaan tenaga yang tinggi. Peningkatan kehilangan penghasilan karbon semasa operasi telah menyebabkan penurunan kecekapan arus dan seterusnya meningkatkan penggunaan tenaga operasi.

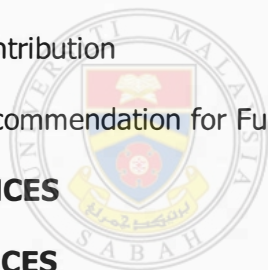
TABLE OF CONTENTS

TITLE	Page
DECLARATION	ii
CERTIFICATION	iii
ACKNOWLEDGEMENT	iv
ABSTRACT	v
<i>ABSTRAK</i>	vi
TABLE OF CONTENTS	vii
LIST OF TABLES	xi
LIST OF FIGURES	xiv
LIST OF ABBREVIATIONS	xxiv
LIST OF SYMBOLS	xxvi
LIST OF APPENDICES	xxvii
CHAPTER 1 INTRODUCTION	1
1.1 Research Background	1
1.2 Problem Statement	3
1.3 Objectives	5
1.4 Scopes of Work	5
CHAPTER 2 LITERATURE REVIEW	8
2.2 Setup and Selection of Electrolysis Equipment and Materials	9
2.2.1 Electrolysis Equipment Setup and Material Selection	9
2.2.2 Electrode Material Selection	11
2.3 Electrolysis Condition	15
2.3.1 CO ₂ Environment in Electrodeposition Process	15

2.3.2	Molten Salt for Electrodeposition Process	16
2.3.3	Electrolysis Temperature	21
2.3.4	Voltage Value and Voltage Feeding	24
2.4	Chemical Reactions Involved in Electrodeposition	29
2.4.1	Reduction Process	29
2.4.2	Oxidation Process	31
2.5	Sample Post Preparation	34
2.6	Carbon Characterisation and Electrodeposition Performance	36
2.6.1	Carbon Purity	36
2.6.2	Carbon Structure Analysis	38
2.6.3	Carbon Crystallinity Analysis	44
2.6.4	Functional Group in Carbon Samples	46
2.6.5	The Electrolysis Efficiency and Energy Consumption	47
CHAPTER 3	METHODOLOGY	50
3.1	Electro Conversion Cell Design and Setup	51
3.1.1	Tube Reactor Setup	52
3.1.2	Reactor System and Furnace Setup	55
3.2	Preparation of The Salt Mixtures	57
3.2.1	Preparation Salt Mixture of $\text{Li}_2\text{CO}_3 - \text{Na}_2\text{CO}_3 - \text{K}_2\text{CO}_3$	58
3.2.2	Preparation Mixture of $\text{CaCO}_3 - \text{Li}_2\text{CO}_3 - \text{LiCl}$	59
3.3	Designing a Custom Made Voltage Feeding Device	60
3.3.1	Continuous Electrolysis Test	61
3.3.2	Gated Pulse Electrolysis Feeding	62
3.3.3	Alternate Terminal Electrolysis Feeding	63
3.4	Electrolysis Operation Setting	64

3.5	Post Preparation of Cathodic Product	65
3.6	Samples Characterisation	68
3.6.1	Composition of The Cathodic Product	69
3.6.2	Carbon Structure Analysis	69
3.6.3	Carbon Crystalline Analysis	71
3.6.4	Surface Functionalising Analysis	72
3.7	Efficiency and Energy Consumption	73
CHAPTER 4 DETERMINATION OF CURRENT POLARISATION AND CARBON ELECTRO-DEPOSITION UNDER VARIOUS VOLTAGE FEEDING		74
4.1	Behaviour of Electrolysis Process Under Different Voltage Feeding	74
4.1.1	$I - t$ Response and Deposition Under Continuous Voltage Feeding	77
4.1.2	$I - t$ Response and Deposition Under Gated Pulse Voltage Feeding	85
4.1.3	$I - t$ Response and Deposition Under Alternate Voltage Feeding	94
4.2	Corrosion of AISI 304 Stainless Steel Electrode	111
4.2.1	Corrosion Attack in Salt Bath $\text{Li}_2\text{CO}_3 - \text{Na}_2\text{CO}_3 - \text{K}_2\text{CO}_3$	112
4.2.2	Corrosion Attack in Salt Bath $\text{CaCO}_3 - \text{Li}_2\text{CO}_3 - \text{LiCl}$	115
CHAPTER 5 CARBON CHARACTERISATION		118
5.1	Carbon Structure Analysis	118
5.1.1	Structures of Carbon Produced in $\text{Li}_2\text{CO}_3 - \text{Na}_2\text{CO}_3 - \text{K}_2\text{CO}_3$	118
5.1.2	Structures of Carbon Produced in $\text{CaCO}_3 - \text{Li}_2\text{CO}_3 - \text{LiCl}$	123
5.2	Carbon Crystalline Structure Analysis	128
5.2.1	Crystalline Structure Analysis for Carbon Prepared in $\text{Li}_2\text{CO}_3 - \text{Na}_2\text{CO}_3 - \text{K}_2\text{CO}_3$	128

5.2.2	Crystalline Structure Analysis for Carbon Prepared in CaCO_3 – Li_2CO_3 – LiCl	131
5.3	Determination of Functional Group in Carbon Samples	133
5.3.1	Functional Group Analysis on Samples Produced in Li_2CO_3 – Na_2CO_3 – K_2CO_3	133
5.3.2	Functional Group Analysis on Samples Produced in CaCO_3 – Li_2CO_3 – LiCl	136
CHAPTER 6 PERFORMANCE OF VOLTAGE FEEDING IN ELECTRO-DEPOSITION PROCESS		138
6.1	Performance of Sample Prepared in Li_2CO_3 – Na_2CO_3 – K_2CO_3	139
6.2	Performance of Sample Prepared in CaCO_3 – Li_2CO_3 – LiCl	144
CHAPTER 7 CONCLUSION AND FUTURE STUDY		150
7.1	Conclusion	150
7.2	Contribution	153
7.3	Recommendation for Future Work	153
REFERENCES		155
APPENDICES		163



UMS
UNIVERSITI MALAYSIA SABAH

LIST OF TABLES

	Page
Table 2.1: Electrode materials for paired electrode that had been used in electrodeposition of carbon in molten contained alkali and earth alkali molten salt	12
Table 2.2: Utilised molten salt in electrochemical conversion of CO ₂ to form carbon	17
Table 2.3: Deposition voltage (vs. CO ₃ ²⁻ /CO ₂ – O ₂) of alkaline metal and carbon in respective molten carbonate salts at 600 °C	20
Table 2.4: Procedure that had been performed by researchers to remove salt residue on the deposits carbon	35
Table 2.5: Elemental composition of deposited product produced under different electrolysis condition at constant cell voltage of 2.2 V	38
Table 3.1: Calculated molar mass of Li ₂ CO ₃ , Na ₂ CO ₃ and K ₂ CO ₃ by given its respective salt molar value	58
Table 3.2: Required mass of Li ₂ CO ₃ , Na ₂ CO ₃ and K ₂ CO ₃ to be prepared	59
Table 3.3: Calculated molar mass by given respective salt molar value	59
Table 3.4: Required mass of CaCO ₃ , Li ₂ CO ₃ and LiCl to be prepared	59
Table 3.5: Set of electrolysis test under gated pulse voltage feeding	63
Table 3.6: Set of electrolysis test under alternate terminal polar voltage feeding.	64

Table 4.1:	The behaviour of the electrodeposition process under continuous voltage feeding in $\text{Li}_2\text{CO}_3 - \text{Na}_2\text{CO}_3 - \text{K}_2\text{CO}_3$	81
Table 4.2:	The behaviour of the electrodeposition process under continuous voltage feeding in $\text{CaCO}_3 - \text{Li}_2\text{CO}_3 - \text{LiCl}$	84
Table 4.3:	The behaviour of the electrodeposition process under gated pulse voltage feeding in $\text{Li}_2\text{CO}_3 - \text{Na}_2\text{CO}_3 - \text{K}_2\text{CO}_3$	89
Table 4.4:	The behaviour of the electrodeposition process under gated pulse voltage feeding in $\text{CaCO}_3 - \text{Li}_2\text{CO}_3 - \text{LiCl}$	93
Table 4.5:	The behaviour of the charge transfer under alternate voltage feeding in $\text{Li}_2\text{CO}_3 - \text{Na}_2\text{CO}_3 - \text{K}_2\text{CO}_3$	97
Table 4.6:	The behaviour of the electrodeposition process alternate voltage feeding in $\text{Li}_2\text{CO}_3 - \text{Na}_2\text{CO}_3 - \text{K}_2\text{CO}_3$	102
Table 4.7:	The behaviour of the charge transfer under alternate voltage feeding in $\text{CaCO}_3 - \text{Li}_2\text{CO}_3 - \text{LiCl}$	106
Table 4.8:	The behaviour of the electrodeposition process under alternate voltage feeding in $\text{CaCO}_3 - \text{Li}_2\text{CO}_3 - \text{LiCl}$	109
Table 4.9	Loss mass of the AISI 304 stainless steel electrode after electrolysis in salt bath $\text{Li}_2\text{CO}_3 - \text{Na}_2\text{CO}_3 - \text{K}_2\text{CO}_3$	112
Table 4.10:	Loss mass of the AISI 304 stainless steel electrode after electrolysis in salt bath $\text{CaCO}_3 - \text{Li}_2\text{CO}_3 - \text{LiCl}$	116

Table 5.1:	Checklist of visibility structures carbon-based constituent in cathodic product produced under different voltage feeding in salt bath $\text{Li}_2\text{CO}_3 - \text{Na}_2\text{CO}_3 - \text{K}_2\text{CO}_3$	123
Table 5.2:	Checklist of visibility structures carbon-based constituent in cathodic product produced under different voltage feeding in salt bath $\text{CaCO}_3 - \text{Li}_2\text{CO}_3 - \text{LiCl}$	128
Table 6.1:	Calculated values of Current Efficiency in % and Energy Consumption in kWh/kg for carbon samples produced in $\text{Li}_2\text{CO}_3 - \text{Na}_2\text{CO}_3 - \text{K}_2\text{CO}_3$ under variation voltage feeding	140
Table 6.2:	Calculated values of Current Efficiency in % and Energy Consumption in kWh/kg for carbon samples produced in $\text{CaCO}_3 - \text{Li}_2\text{CO}_3 - \text{LiCl}$ under variation voltage feeding	145



UMS
UNIVERSITI MALAYSIA SABAH

LIST OF FIGURES

	Page
Figure 2.1: Experimental setup of producing solid carbon deposition electrochemical conversion of CO ₂ to carbon. (a) schematic setup and (b) actual setup.	10
Figure 2.2: Non-scaled concept design of the electrolysis cell reactor with three electrode arrangements.	11
Figure 2.3: Condition of nickel anode in 4.0 V electrochemical conversion of CO ₂ to carbon in molten Li ₂ CO ₃ – K ₂ CO ₃ (mole ratio 0.5:0.5) electrolysis at 544 – 547 °C. (a) after one hour electrolysis and (b) after 14 hours electrolysis.	13
Figure 2.4: Degradation of SnO ₂ electrode in 4.0 V electrochemical conversion of CO ₂ to carbon in molten Li ₂ CO ₃ – K ₂ CO ₃ (mole ratio 0.5:0.5) electrolysis at 544 – 547 °C.	14
Figure 2.5: Behaviour of SS 304 anode electrode in 4.0 V electrochemical conversion of CO ₂ to carbon in molten Li ₂ CO ₃ – K ₂ CO ₃ (mole ratio 0.5:0.5) electrolysis at 544 – 547 °C.	15
Figure 2.6: Effects of various CO ₂ partial pressure on the carbon deposition rate.	16
Figure 2.7: The phase diagram of Li ₂ CO ₃ – Na ₂ CO ₃ binary salt mixtures with increasing mole of Na ₂ CO ₃ .	22
Figure 2.8: The phase diagram of Li ₂ CO ₃ – K ₂ CO ₃ binary salt mixtures with increasing mole of Li ₂ CO ₃ .	23

Figure 2.9:	The phase diagram of LiCl – Li ₂ CO ₃ binary salt mixtures with increasing mole of Li ₂ CO ₃ .	24
Figure 2.10:	Current – time plots of the electrolysis in molten mixture of Li ₂ CO ₃ – Na ₂ CO ₃ – K ₂ CO ₃ (mole ratio 43.5:31.5:25.0) at temperature 550 °C.	25
Figure 2.11:	Electrical circuit for basic concept of DC pulse voltage generator.	26
Figure 2.12:	Current – time plot obtained in an electrolysis using polarity reversal technique in molten LiCl at temperature 775 °C; cathodic voltage -2.5 V vs Mo reference electrode with switching interval 1 min and total duration is 20 min ('A' and 'B' represent segment of different polarity).	27
Figure 2.13:	Carbon deposition produced at 4.0 V cell voltage, under CO ₂ environment (a) in 544 – 547 °C molten salt mixture of Li ₂ CO ₃ -K ₂ CO ₃ (1:1 mole ratio); (b) in 579 °C molten salt mixture CaCl ₂ – CaCO ₃ – LiCl – KCl (0.13:0.31:0.45:0.13 mole ratio).	30
Figure 2.14:	Comparison Gibbs energy of the: $2\text{CO}_3^{2-} \rightarrow 2\text{CO}_2 + \text{O}_2 + 4\text{e}^-$; $2\text{O}^{2-} \rightarrow \text{O}_2 + 4\text{e}^-$; and $2\text{Cl}^- \rightarrow \text{Cl}_2 + 2\text{e}^-$.	32
Figure 2.15:	Electrochemical dissociation of different (a) carbonate salts and (b) chloride salts of alkali/earth alkali metal.	33
Figure 2.16:	EDX spectrum of the deposited products obtained under cell voltage 4.5 V at 550 °C in Li ₂ CO ₃ – Na ₂ CO ₃ – K ₂ CO ₃ (mole % ratio 43.5:31.5:25.0).	37

Figure 2.17:	TEM image of aggregated particulates structure found in deposited carbon that prepared with 4.0 V in molten Li_2CO_3 at 740 °C under the CO_2 atmosphere.	39
Figure 2.18:	SEM images of carbon powder obtained under constant cell voltage 4.0 V at (a) 550 °C and (b) 650 °C, in molten mixture $\text{Li}_2\text{CO}_3 - \text{Na}_2\text{CO}_3 - \text{K}_2\text{CO}_3$ (mole % ratio 43.5:31.5:25.0).	40
Figure 2.19:	TEM image of carbon flake structure found in deposited carbon that prepared with 4.0 V in molten Li_2CO_3 at 740 °C under the CO_2 atmosphere.	41
Figure 2.20:	SEM image of MWCNTs at higher magnification in carbon specimen.	42
Figure 2.21:	TEM image of MWCNTs from the carbon specimen which was prepared via reversal electrolysis polarity technique.	42
Figure 2.22:	TEM image of MWCNTs from the carbon specimen that prepared via electrochemical conversion of CO_2 in molten $\text{Na,K,Cs Cl} - \text{CO}_2$ (15 atm) at 550 °C.	43
Figure 2.23:	TEM images of carbon nano powders deposited in molten $\text{Li}_2\text{CO}_3 - \text{Na}_2\text{CO}_3 - \text{K}_2\text{CO}_3$ at 450 °C and annealed at 600 °C.	43
Figure 2.24:	XRD diffraction patterns of the annealed carbon that obtained under constant 4.0 V drive electrolysis at indicated molten temperature.	44
Figure 2.25:	XRD diffraction patterns of the carbon products deposited in molten $\text{Li}_2\text{CO}_3 - \text{Na}_2\text{CO}_3 - \text{K}_2\text{CO}_3$ at 550 °C, at indicated voltages.	45

Figure 2.26:	XRD diffraction patterns of the carbon products deposited in molten $\text{Li}_2\text{CO}_3 - \text{K}_2\text{CO}_3$ at indicated voltages and temperatures.	46
Figure 2.27:	FTIR spectra containing different concentration of carbon black in acrylonitrile butadiene rubber.	47
Figure 2.28:	Energy consumption and current efficiency under different cell voltage in molten $\text{Li}_2\text{CO}_3 - \text{Na}_2\text{CO}_3 - \text{K}_2\text{CO}_3$ at temperature (a) 450 °C, (b) in 550 °C, (c) 650 °C.	48
Figure 3.1:	Flow of the designed experimental work.	50
Figure 3.2:	Experimental setup (a) the schematic diagram of molten salt electrochemical cell reactor and (b) the actual experimental setup.	51
Figure 3.3:	The installation features of tube reactor.	53
Figure 3.4:	Main body of the designed cell lid.	54
Figure 3.5:	Full features setup of the Lid cell.	55
Figure 3.6:	The installation of the lid cell on the tube reactor.	56
Figure 3.7:	(a) Actual connection of DPDT switch to DC power supply and (b) the features of the DPDT switch at open circuit mode.	60
Figure 3.8:	The circuit diagram for continuous voltage feeding drive electrolysis test with DPDT.	61

Figure 3.9:	(a) The circuit diagram for gated pulsed voltage feeding drive electrolysis process with DPDT and (b) its voltage output.	62
Figure 3.10:	Circuit diagram concept of electrolysis test under alternate terminal polar voltage feeding drive electrochemical reaction with DPDT.	63
Figure 3.11:	Deposited carbon or cathodic product immersed in diluted HCl under stirred condition.	66
Figure 3.12:	Filtration of cathodic product or carbon deposits after removal of the salt residue.	67
Figure 3.13:	Washing process of removing HCl residue by using plenty amount of distilled water.	67
Figure 3.14:	The filtered cathodic product on the filter paper.	68
Figure 3.15:	The example of powder sample held by double sided tape on the SEM stub.	69
Figure 3.16:	The loading area of the cathodic sample for analysis on the ATRFTIR equipment.	72
Figure 4.1:	The recorded electrolysis time and current due to in salt $\text{Li}_2\text{CO}_3 - \text{Na}_2\text{CO}_3 - \text{K}_2\text{CO}_3$ under continuous voltage feeding.	75
Figure 4.2:	$I - t$ plot for electrolysis under continuous voltage feeding in salt of $\text{Li}_2\text{CO}_3 - \text{Na}_2\text{CO}_3 - \text{K}_2\text{CO}_3$.	78
Figure 4.3:	Progression of the deposition growth under continuous voltage feeding.	79

Figure 4.4:	The black deposit on stainless steels AISI 304 cathode electrode produced in salt bath $\text{Li}_2\text{CO}_3 - \text{Na}_2\text{CO}_3 - \text{K}_2\text{CO}_3$.	80
Figure 4.5:	I – t plot for electrolysis under continuous voltage feeding in salt of $\text{CaCO}_3 - \text{Li}_2\text{CO}_3 - \text{LiCl}$.	82
Figure 4.6:	The black deposit on stainless steels AISI 304 cathode electrode produced in salt bath $\text{CaCO}_3 - \text{Li}_2\text{CO}_3 - \text{LiCl}$.	83
Figure 4.7:	Polarisation output for electrolysis under gated pulsed voltage feeding salt bath of $\text{Li}_2\text{CO}_3 - \text{Na}_2\text{CO}_3 - \text{K}_2\text{CO}_3$.	86
Figure 4.8:	Progression of the deposition growth under gated pulsed voltage feeding.	87
Figure 4.9:	Deposition of cathodic product under gated pulsed voltage feeding in salt bath $\text{Li}_2\text{CO}_3 - \text{Na}_2\text{CO}_3 - \text{K}_2\text{CO}_3$.	88
Figure 4.10:	Polarisation output for electrolysis under gated pulsed voltage feeding salt bath of $\text{CaCO}_3 - \text{Li}_2\text{CO}_3 - \text{LiCl}$.	91
Figure 4.11:	Deposition of cathodic product under gated pulsed voltage feeding in molten mixture of $\text{CaCO}_3 - \text{Li}_2\text{CO}_3 - \text{LiCl}$.	92
Figure 4.12:	Polarisation output of alternated terminal polar voltage feeding under controlled duration of ramping polar position in salt bath $\text{Li}_2\text{CO}_3 - \text{Na}_2\text{CO}_3 - \text{K}_2\text{CO}_3$.	96
Figure 4.13:	Progression of the deposition growth under alternate voltage feeding.	98

Figure 4.14:	Dense cathodic deposition product under alternate voltage feeding in molten $\text{Li}_2\text{CO}_3 - \text{Na}_2\text{CO}_3 - \text{K}_2\text{CO}_3$.	100
Figure 4.15:	The collected cathodic slurry from deposited product in carbon collector after undergoes 3.0 hours alternated voltage feeding with ramping position (5:5) in molten salt bath $\text{Li}_2\text{CO}_3 - \text{Na}_2\text{CO}_3 - \text{K}_2\text{CO}_3$.	101
Figure 4.16:	Polarisation output of alternated terminal polar voltage feeding under controlled duration of ramping polar position in salt bath $\text{CaCO}_3 - \text{Li}_2\text{CO}_3 - \text{LiCl}$.	104
Figure 4.17:	Cathodic deposition product with fine crater like surface produced under alternate voltage feeding in molten mixture of $\text{CaCO}_3 - \text{Li}_2\text{CO}_3 - \text{LiCl}$.	107
Figure 4.18:	The collected felled deposition fragment from deposited product in carbon collector after undergoes 3.0 hours alternated voltage feeding with ramping position (5:10) in molten salt bath $\text{CaCO}_3 - \text{Li}_2\text{CO}_3 - \text{LiCl}$.	108
Figure 4.19:	The surface condition of the electrodes SSE2 and SSE1 surfaces after 3.0 hours electrolysis under alternate voltage feeding in salt bath $\text{Li}_2\text{CO}_3 - \text{Na}_2\text{CO}_3 - \text{K}_2\text{CO}_3$.	114
Figure 4.20:	The surface condition of the electrodes SSE1 and SSE2 surfaces after 3.0 hours electrolysis under alternate voltage feeding at positioning ramping ratio (10:10) in salt bath $\text{CaCO}_3 - \text{Li}_2\text{CO}_3 - \text{LiCl}$.	117
Figure 5.1:	SEM images of (a) particulates, (b) flake, and (c) honeycomb-like carbon structures, and the EDX elemental composition	119

for sample produced in molten salt bath mixture of Li_2CO_3 – Na_2CO_3 – K_2CO_3 under continuous and gated pulse voltage feeding.

- Figure 5.2: TEM image of carbon structure with rhombus shape in sample prepared in salt bath Li_2CO_3 – Na_2CO_3 – K_2CO_3 under continuous voltage feeding. 120
- Figure 5.3: SEM images of (a) cotton and (b) tread – like carbon structures, and the EDX elemental composition for sample produced in molten salt bath mixture of Li_2CO_3 – Na_2CO_3 – K_2CO_3 under alternate voltage feeding. 121
- Figure 5.4: TEM image of crystal nanoparticle shape in cathodic sample prepared in Li_2CO_3 – Na_2CO_3 – K_2CO_3 under the alternate voltage feeding. 122
- Figure 5.5: TEM image on CNT structure found in samples produced under the alternate voltage feeding in molten salt bath of Li_2CO_3 – Na_2CO_3 – K_2CO_3 . 122
- Figure 5.6: Example of SEM images of (a) particulate, (b) flake and (c) tube structures, and the EDX elemental composition for carbon produced in molten salt bath mixture of CaCO_3 – Li_2CO_3 – LiCl under continuous and gated pulse voltage feeding. 124
- Figure 5.7: TEM image of carbon with flake structure in sample prepared in CaCO_3 – Li_2CO_3 – LiCl under continuous voltage feeding. 125

Figure 5.8:	SEM images of tube structure and the EDX elemental composition for carbon produced in molten salt bath mixture of $\text{CaCO}_3 - \text{Li}_2\text{CO}_3 - \text{LiCl}$ under alternate voltage feeding.	126
Figure 5.9:	TEM images on CNT structure found in samples produced under (a) continuous voltage feeding, (b) gated pulse voltage feeding (GP20'), and (c) alternate voltage feeding ($t_{p1}:t_{p2} = 10:5$) in $\text{CaCO}_3 - \text{Li}_2\text{CO}_3 - \text{LiCl}$.	127
Figure 5.10:	XRD patterns of the cathodic product that being produced in salt bath $\text{Li}_2\text{CO}_3 - \text{Na}_2\text{CO}_3 - \text{K}_2\text{CO}_3$ under continuous and gated pulsed voltage feeding.	129
Figure 5.11:	XRD patterns of the cathodic product that being produced in salt bath $\text{Li}_2\text{CO}_3 - \text{Na}_2\text{CO}_3 - \text{K}_2\text{CO}_3$ under alternate voltage feeding.	130
Figure 5.12:	XRD patterns of the cathodic product that being produced in salt bath $\text{CaCO}_3 - \text{Li}_2\text{CO}_3 - \text{LiCl}$ under continuous and gated pulsed voltage feeding.	131
Figure 5.13:	XRD patterns of the cathodic product that being produced in salt bath $\text{CaCO}_3 - \text{Li}_2\text{CO}_3 - \text{LiCl}$ under alternate voltage feeding.	132
Figure 5.14:	FTIR spectra of carbon sample produced in $\text{Li}_2\text{CO}_3 - \text{Na}_2\text{CO}_3 - \text{K}_2\text{CO}_3$ under (a) continuous and gated pulse and (b) alternate voltage feeding.	134
Figure 5.15:	FTIR spectra of carbon sample produced in $\text{CaCO}_3 - \text{Li}_2\text{CO}_3 - \text{LiCl}$ under (a) continuous and gated pulse and (b) alternate voltage feeding.	136

Figure 6.1: (a) Theoretical and actual yield carbon, (b) Current efficiency 142
and (c) Energy to produced 1 kg of carbon via electrolysis
process in $\text{Li}_2\text{CO}_3 - \text{Na}_2\text{CO}_3 - \text{K}_2\text{CO}_3$ under variation of voltage
feeding.

Figure 6.2: (a) Theoretical and actual yield carbon, (b) Current efficiency 146
and (c) Energy to produced 1 kg of carbon via electrolysis
process in $\text{CaCO}_3 - \text{Li}_2\text{CO}_3 - \text{LiCl}$ under variation of voltage
feeding.



UMS
UNIVERSITI MALAYSIA SABAH

LIST OF ABBREVIATIONS

- A1** - Sample Alternate 1 for $\text{Li}_2\text{CO}_3 - \text{Na}_2\text{CO}_3 - \text{K}_2\text{CO}_3$
- A1'** - Sample Alternate 1 for $\text{CaCO}_3 - \text{Li}_2\text{CO}_3 - \text{LiCl}$
- ATR** - Attenuated Total Reflection
- CCM** - Close Circuit Mode
- CCS** - Carbon Capture and Storage
- CCU** - Carbon Capture and Utilisation
- CCSU** - Carbon Capture Storage and Utilisation
- CNP** - Carbon Nano-Particle
- CNT** - Carbon Nano-Tube
- COM 1** - Communication point 1 for DPDT
- Cont.** - Sample Continuous for $\text{Li}_2\text{CO}_3 - \text{Na}_2\text{CO}_3 - \text{K}_2\text{CO}_3$
- Cont.'** - Sample Continuous for $\text{CaCO}_3 - \text{Li}_2\text{CO}_3 - \text{LiCl}$
- CT1** - Cell terminal 1
- DPDT** - Double Pole Double Throw
- EA** - Elemental Analyser